

Ionization of hydrogen atoms by electron impact at 1eV, 0.5eV and 0.3eV above threshold

J. N. Das and S. Paul

*Department of Applied Mathematics, University College of Science, 92, Acharya
Prafulla Chandra Road, Calcutta - 700 009, India*

K. Chakrabarti

*Department of Mathematics, Scottish Church College, 1 & 3 Urquhart Square,
Calcutta - 700 006, India*

Abstract

We present here cross section results for ionization of hydrogen atoms by electron impact at 1eV, 0.5eV and 0.3eV energy above threshold, calculated in hyperspherical partial wave theory. The results are in excellent agreement with the available semiclassical results of Crothers *et al* [2002] for these energies. Considering its success above 1eV energy [Das *et al* (2003)] for various kinematic conditions, and considering the present success some advantages of the hyperspherical partial wave theory over other sophisticated theories, requiring large scale computations, are clearly demonstrated.

e-mail : jndas@cucc.ernet.in

I. Introduction

Over the last couple of years considerable progress has been made in the study of ionization of hydrogen atoms by electron impact, apparently the simplest three body coulomb problem in quantum scattering theory at low energies. Still full understanding of this problem, particularly near threshold, has not been achieved. For equal-energy-sharing kinematics McCurdy and co-workers made a break-through calculation in their exterior complex scaling (ECS) approach [Rescigno *et al*(1999)]. Their results for 30eV, 25eV, 19.6eV and 17.6eV, surprisingly agree, particularly qualitatively, with the measured results of Röder *et al*[1997,2002]. But below 2eV, results of ECS theory are not yet available. ECS approach needs huge computational resources and special numerical techniques. Below 2eV energy ECS approach may need far more computational resources. Another sophisticated approach is the convergent close-coupling (CCC) theory of Bray and associates [1994], which works so beautifully for other atomic scattering problems, reproduces ionization cross section results satisfactorily only above 2eV excess energy. For 2eV excess energy their results differ significantly from the absolute measured values [Röder *et al*(1997)]. Below 2eV excess energy CCC results are also not available. Recent calculations of Das and co-workers, in the hyperspherical partial wave theory (HSPW), for equal-energy-sharing kinematics, when the two outgoing electrons have equal energies, also works nicely [Das et al 2003]. So far hyperspherical partial wave theory has not been tested below 2eV excess energy. Very recently semiclassical calculations of Crothers and co-workers has been reported [2002], which gives very good cross section results for low energies, say 4eV and 2eV excess energies. Their results for 1eV, 0.5eV and 0.3eV excess energies are also available. This calculation encouraged us to test whether the hyperspherical partial wave theory works for excess energy below 2eV. Here we made such a test for excess energy of 1eV, 0.5eV and 0.3eV. We find surprisingly that the HSPW theory really gives excellent cross section results in very good agreement with the semi classical calculation of Crothers *et al*[2002] for the above very low energies. Here we only need to increase the asymptotic range parameter R_∞ to sufficiently large values of several thousands of a.u. for these energies, possibly not thinkable in ECS calculations. It may be noted here that in the hyperspherical R-matrix with semiclassical outgoing waves(HRM-SOW) calculations of Selles *et al*[2002] for double photo-ionization of Helium also needed values of R_∞ thousands of a.u. for converged results.

II. Hyperspherical Partial Wave Theory

Hyperspherical partial wave theory has been described in details in [Das 1998, Das *et al* 2003] and briefly in [Das 2001 and Das 2002]. In this approach we determine

scattering amplitude from the T-matrix element given by

$$T_{fi} = \langle \Psi_f^{(-)} | V_i | \Phi_i \rangle \quad (1)$$

where Φ_i is the initial state wave function, V_i is the interaction potential in this channel and $\Psi_f^{(-)}$ is the exact two-electron continuum wave function with incoming boundary conditions, in presence of the nucleus, which is considered infinitely heavy and sitting at the origin. The scattering state $\Psi_f^{(-)}$ is determined by expanding it in terms of symmetrized hyperspherical harmonics [Das 1998, Lin 1974] which are functions of five angular variables. The hyper radius and the angular variables are defined by $R = \sqrt{r_1^2 + r_2^2}$, $\alpha = \text{atan}(r_2/r_1)$, $\hat{r}_1 = (\theta_1, \phi_1)$, $\hat{r}_2 = (\theta_2, \phi_2)$ and $\omega = (\alpha, \hat{r}_1, \hat{r}_2)$ and set $P = \sqrt{p_1^2 + p_2^2}$, $\alpha_0 = \text{atan}(p_2/p_1)$, $\hat{p}_1 = (\theta_{p_1}, \phi_{p_1})$, $\hat{p}_2 = (\theta_{p_2}, \phi_{p_2})$ and $\omega_0 = (\alpha_0, \hat{p}_1, \hat{p}_2)$, \vec{p}_1 , \vec{p}_2 being momenta of the two outgoing electrons of energies E_1 and E_2 , and positions \vec{r}_1 and \vec{r}_2 .

Different sets of radial waves with definite $\mu = (L, S, \pi)$, where L is the total angular momentum, S is total spin and π is the parity, satisfy different sets of coupled equations each of the form

$$\left[\frac{d^2}{dR^2} + P^2 - \frac{\nu_N (\nu_N + 1)}{R^2} \right] f_N + \sum_{N'} \frac{2P \alpha_{NN'}}{R} f_{N'} = 0. \quad (2)$$

These equations are truncated to $N = N_{mx}$, the number of channels retained in the calculation for each fixed μ . The N_{mx} number of independent solutions of the truncated equations, have to be determined over the interval $(0, \infty)$. This equations may be solved in different alternative approaches [Das 2001, 2002, Das *et al* 2003]. The most effective approach turns out to be the one in which the interval $(0, \infty)$ is divided into three subintervals $(0, \Delta)$, (Δ, R_∞) and (R_∞, ∞) , where Δ is of few atomic units and R_∞ is some point in the far asymptotic domain. One may construct N_{mx} independent solutions of equations (2) over $(0, \Delta)$ by solving these as a two-points boundary value problem, the k-th solution vector is made to vanish at the origin and take the k-th column of the $N_{mx} \times N_{mx}$ unit matrix as its value at Δ . These solutions are then continued over (Δ, R_∞) by solving these equations by the Taylor's expansion method with frequent stabilization. Beyond R_∞ the solution may be obtained from expansion in inverse powers of R with suitable sine and cosine factors [Das 1998, Das *et al* 2003]. Then the asymptotic incoming boundary conditions completely define [Das 1998, Das *et al* 2003] the scattering-states wave function $\Psi_{fs}^{(-)}$. For the initial interval $(0, \Delta)$ solution by the difference method proves most effective. In our earlier calculation [Das *et al* 2003], at higher energies we used a five-point difference scheme. This gives us very good cross sections for 30eV, 25eV, 19.6eV and 17.6eV for varied kinematic conditions. In our present calculation we propose to use larger mesh size (double of our previous calculation). So in place of a five-point difference scheme we use a seven-point difference scheme as described below.

In the seven-point scheme we divide the interval $[0, \Delta]$ into m subintervals by using mesh points $R_0, R_1, R_2, \dots, R_{m-1}, R_m$ where $R_k = hk$, $k = 0, 1, 2, \dots, m$ and $h = \Delta/m$.

In this scheme we use the following formulae

$$f''_N(R_k) = \frac{1}{h^2} \left[\frac{1}{90} f_N(R_{k-3}) - \frac{3}{20} 16 f_N(R_{k-2}) + \frac{3}{2} f_N(R_{k-1}) - \frac{49}{18} f_N(R_k) + \frac{3}{2} f_N(R_{k+1}) - \frac{3}{20} 16 f_N(R_{k+2}) + \frac{1}{90} f_N(R_{k+3}) \right] + \left\{ \frac{69}{25200} h^6 f_N^{(viii)}(\xi_1) \right\} \quad (3)$$

for $k = 3, 4, \dots, m-4, m-3$, and for $k = 1, 2$ and $m-2, m-1$ the formulae

$$f''_N(R_1) = \frac{1}{h^2} \left[\frac{3}{8} f_N(R_0) + 6 f_N(R_1) - \frac{11}{2} h^2 f''_N(R_2) - \frac{51}{4} f_N(R_3) - h^2 f''_N(R_3) + 6 f_N(R_4) + \frac{3}{8} f_N(R_4) \right] + \left\{ -\frac{23}{10080} h^6 f^{(viii)}(\xi_2) \right\}. \quad (4)$$

$$f''_N(R_2) = \frac{1}{h^2} \left[\frac{3}{8} f_N(R_1) + 6 f_N(R_2) - \frac{11}{2} h^2 f''_N(R_3) - \frac{51}{4} f_N(R_3) - h^2 f''_N(R_4) + 6 f_N(R_4) + \frac{3}{8} f_N(R_5) \right] + \left\{ -\frac{23}{10080} h^6 f^{(viii)}(\xi_3) \right\}. \quad (5)$$

$$f''_N(R_{m-2}) = \frac{1}{h^2} \left[\frac{3}{8} f_N(R_{m-5}) + 6 f_N(R_{m-4}) - h^2 f''_N(R_{m-4}) - \frac{51}{4} f_N(R_{m-3}) - \frac{11}{2} h^2 f''_N(R_{m-3}) + 6 f_N(R_{m-2}) + \frac{3}{8} f_N(R_{m-1}) \right] + \left\{ -\frac{23}{10080} h^6 f^{(viii)}(\xi_4) \right\}. \quad (6)$$

and

$$f''_N(R_{m-1}) = \frac{1}{h^2} \left[\frac{3}{8} f_N(R_{m-4}) + 6 f_N(R_{m-3}) - h^2 f''_N(R_{m-3}) - \frac{51}{4} f_N(R_{m-2}) - \frac{11}{2} h^2 f''_N(R_{m-2}) + 6 f_N(R_{m-1}) + \frac{3}{8} f_N(R_m) \right] + \left\{ -\frac{23}{10080} h^6 f^{(viii)}(\xi_5) \right\}. \quad (7)$$

The quantities on the right hand sides within curly brackets represent the error terms. The corresponding difference equations are obtained by substituting these expressions the values of second order derivatives from the differential equation (12). For continuing these solutions in the domain (Δ, R_∞) we need first order derivatives $f'_N(R)$ at Δ . These are computed from the difference formula

$$f'_N(R_m) = \frac{1}{84h} [-f_N(R_{m-4}) + 24f_N(R_{m-2}) - 128f_N(R_{m-1}) + 105f_N(R_m)] + \frac{2h}{7} f''_N(R_m) + \left\{ -\frac{4h^4}{105} f_N^{(v)}(\xi) \right\} \quad (8)$$

Here too, the quantity within curly brackets represents the error term. The solutions thus obtained in $(0, \Delta)$ are then continued over (Δ, R_∞) by Taylor's expansion method, as stated earlier, with stabilization after suitable steps [Choi and Tang 1975].

III. Results

In our present calculation for the equal-energy-sharing kinematics for 1eV, 0.5eV and 0.3eV excess energies, we have included 30 channels and have chosen $\Delta = 5$ a.u. (as in our previous calculation [Das *et al* 2003] for higher energies). Small variation of the value of Δ about the value chosen does not change the results. Here we need to chose R_∞ of about 1000 a.u. for 1eV, 2000 a.u. for 0.5eV and 3000 a.u. for 0.3eV for smooth convergence of the asymptotic series solution and for smooth fitting with the asymptotic solution [Das *et al* 2003] for equal-energy-sharing cases. For unequal-energy-sharing cases one has to move to still larger distances. For going to the far asymptotic domain a larger value of h (grid spacing) is preferable. Here we have chosen $h = 0.1$ a.u. up to Δ and a value 0.2 a.u. beyond Δ in all the cases. Accordingly a seven point scheme, as described above, is more suitable over a five point scheme used in our earlier calculation [Das *et al* 2003]. So we have chosen the above seven-point scheme in the present calculation. In our present calculations we included states with L up to 5. Values of L above 5 give insignificant contributions. The (l_1, l_2) pairs which have been included in our calculation are more or less sufficient for near convergence as is evident from the results of calculations with the inclusion of larger number of channels. Computation with all these have been easily carried out on a 2 CPU SUN Enterprise 450 system with 512 MB RAM (However the calculation could not be done on a Pentium-III PC).

For each incident energy three sets of results have been presented for the two outgoing electrons having equal energies. These are constant - Θ_{ab} geometry results, Θ_a -constant geometry results and the results for symmetric geometry. For 1eV excess energy we have presented these results in figures 1(a),1(b) and 1(c) respectively. The corresponding results for energy 0.5eV are presented in figures 2(a),2(b) and 2(c) respectively. The results for 0.3eV have been presented in figures 3(a),3(b) and 3(c) respectively. Here we compare our results with the very recent semiclassical calculation of Crothers *et al* [2002] for $\Theta_{ab} = 180^\circ$ and 150° in figures 1(a),2(a) and 3(a). For other geometries, unfortunately, neither experimental nor any theoretical results are available for comparison. In any case the close agreement between our results and those of Deb and Crothers for $\Theta_{ab} = 180^\circ$ and $\Theta_{ab} = 150^\circ$ is highly encouraging and the results are likely to be very good. A little steeper rise of our results compared to those of Deb and Crothers at 0° are in conformity with the general trends of our corresponding earlier results [Das *et al* 2003] for 2eV and 4eV excess energies. Our results for $\Theta_{ab} = 120^\circ$ and 100° also appear good. Unfortunately there are no experimental results for verification. The results for Θ_a -constant geometry and those of symmetric geometry are also in very nice agreement in shapes, particularly for $\Theta_a = -30^\circ$ and $\Theta_a = -150^\circ$, with those for 2eV and 4eV excess energy cases (see Das *et al* [2003]). The absolute experimental results for these geometries at 2eV and 4eV excess energies also suggest that our present results are likely to be accurate.

IV. Conclusions

From the results presented above it may be claimed that the hyperspherical partial wave theory works at 1eV,0.5eV and 0.3eV excess energies also. We have already good results [Das *et al* 2003] for energies up to 30eV for various kinematic conditions. Inclusion of states with angular momentum, say up to 15, give correct cross sections at higher energies, say 54.4eV or 60eV (such calculations are now in progress). For extreme unequal-energy-sharing cases, calculations with larger values of R_∞ , compared to those for equal-energy-sharing cases are likely to give dependable results for such kinematical conditions also. Another point to note is that in this approach exploration of far asymptotic domain is possible by increasing R_∞ to thousands of atomic units, which is possibly not thinkable for ECS or similar other calculations. All these suggest that the hyperspherical partial wave theory has some advantages over existing other very sophisticated calculations requiring large scale computations. We expect that experimental results at 1eV,0.5eV and 0.3eV excess energies will give further support to our claim.

V. ACKNOWLEDGMENTS

One of the authors (S.Paul) is grateful to CSIR for providing a research fellowship.

References

- [1] Baertschy M, Rescigno T N, Isaacs W A, Li X and McCurdy C W 2001 Phys. Rev. A **63** 022712.
- [2] Baertschy M , Rescigno T N and McCurdy C W 2001 Phys. Rev. A**64** 022709.
- [3] Bray I, Konovalov D A, McCarthy I E and Stelbovics A T 1994 Phys. Rev. A**50** R2818.
- [4] Bray I 1999 J. Phys. B **32** L119 ; 2000 J. Phys. B **33** 581.
- [5] Bray I, 2000 J. Phys. B **33** 581.
- [6] Choi B H and Tang K T 1975 J.Chem.Phys. **63** 1775.
- [7] Crothers D S F 1986 J. Phys. B **19** 463.
- [8] Das J N 1998 Pramana- J. Phys. **50** 53.
- [9] Das J N 2001 Phys. Rev. A **64** 054703.
- [10] Das J N 2002 J. Phys. B **35** 1165.
- [11] Das J N, Paul S and Chakrabarti K 2003 Phys. Rev. A **67** 042717.
- [12] Deb N C and Crothers D S F 2002 Phys. Rev. A **65** 052721.
- [13] Lin C D 1974 Phys. Rev. A **10** 1986.
- [14] Rescigno T N, Baertschy M, Isaacs W A, and McCurdy C W 1999 Science **286** 2474.
- [15] Röder J, Rasch J, Jung K, Whelan C T, Ehrhardt H, Allan R J,Walters H R J 1996 Phys. Rev. A **53** 225.
- [16] Röder J, Ehrhardt H, Pan C, Starace A F, Bray I, and Fursa D 1997 Phys. Rev. Lett. **79** 1666.
- [17] Röder J, Baertschy M and Bray I 2002 Phys. Rev A **45** 2951 (to be published).
- [18] Selles P, Malegat L and Kazansky A K 2002 Phys. Rev. A**65** 032711.

Figure Captions

Figure 1(a). TDCS for coplanar equal-energy-sharing constant Θ_{ab} geometry at 1eV excess energy above threshold. Continuous curves, present results ; dashed-curves, semi-classical results of Deb and Crothers [2002]

Figure 1(b). TDCS for coplanar equal-energy-sharing geometry at 1eV excess energy above threshold for fixed θ_a and variable θ_b of the out going electrons.

Figure 1(c). TDCS for coplanar equal-energy-sharing with two electrons emerging on opposite sides of the direction of the incident electron with equal angle θ_a at 1eV excess energy above threshold.

Figure 2(a). Same as in figure 1(a) but for 0.5eV excess energy.

Figure 2(b). Same as in figure 1(b) but for 0,5eV excess energy.

Figure 2(c). Same as in figure 1(c) but for 0.5eV excess energy.

Figure 3(a). Same as in figure 1(a) but for 0.3eV excess energy.

Figure 3(b). Same as in figure 1(b) but for 0,3eV excess energy.

Figure 3(c). Same as in figure 1(c) but for 0.3eV excess energy.

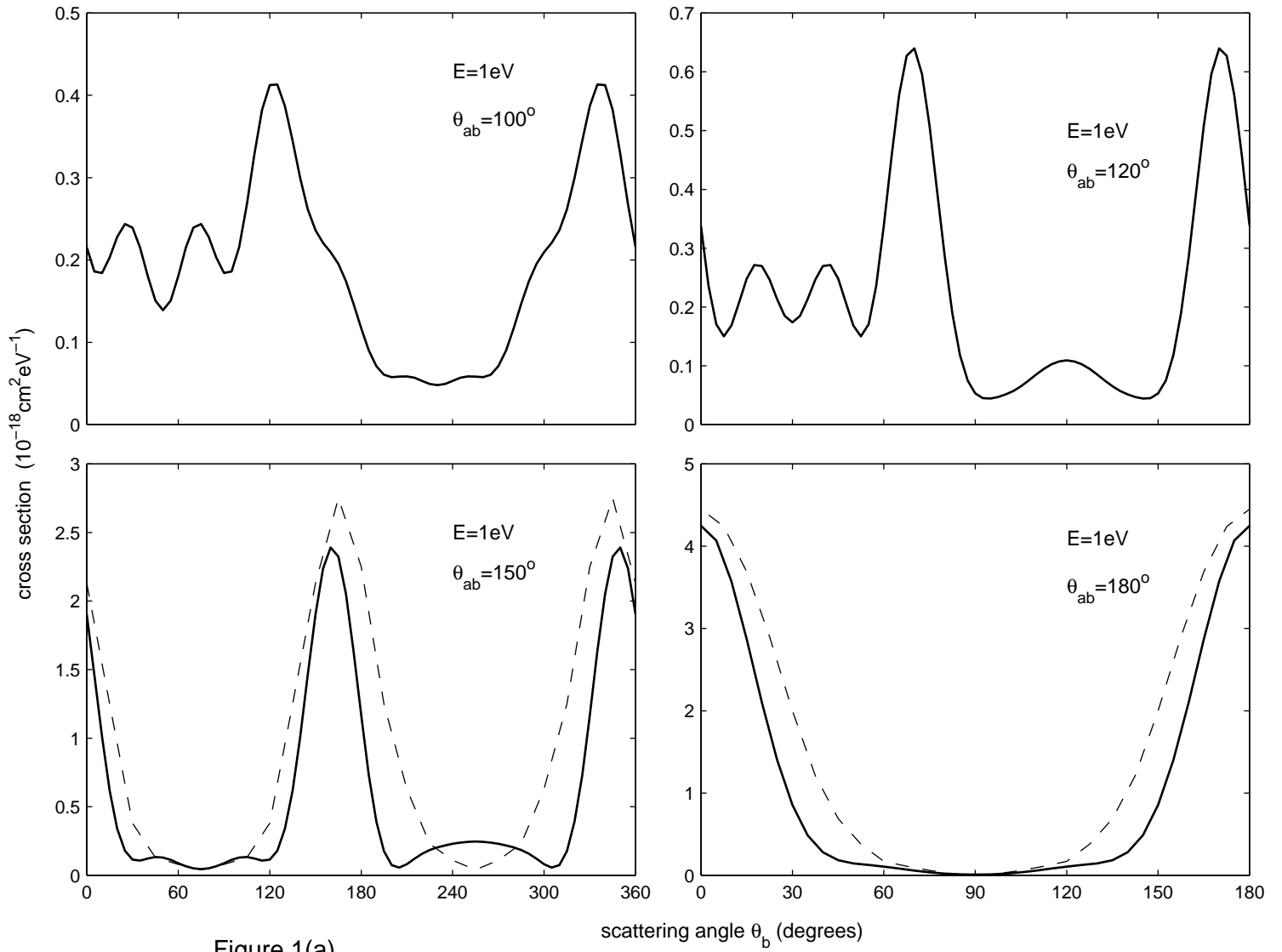


Figure 1(a)

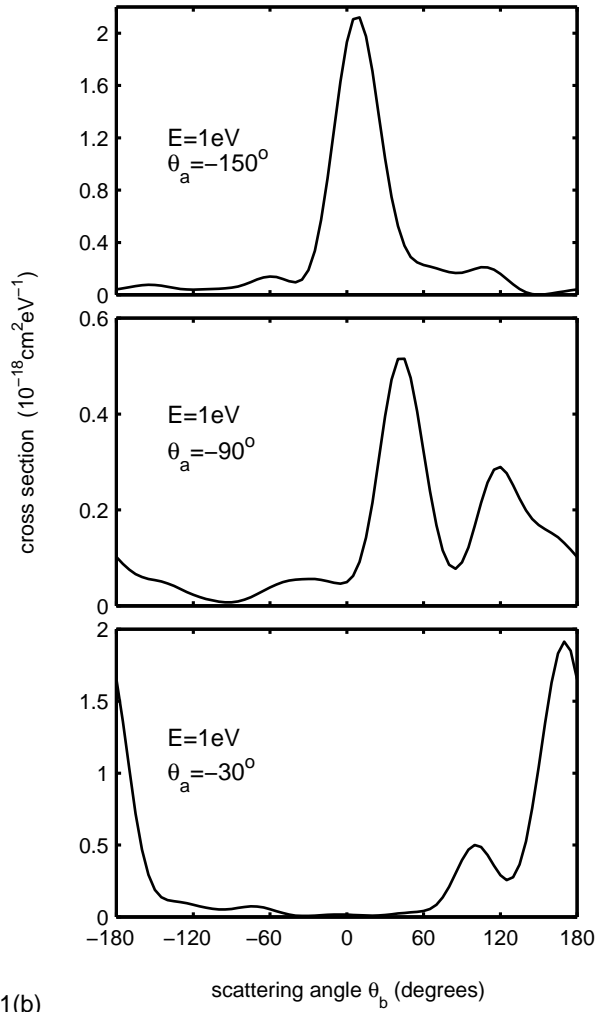


Figure 1(b)

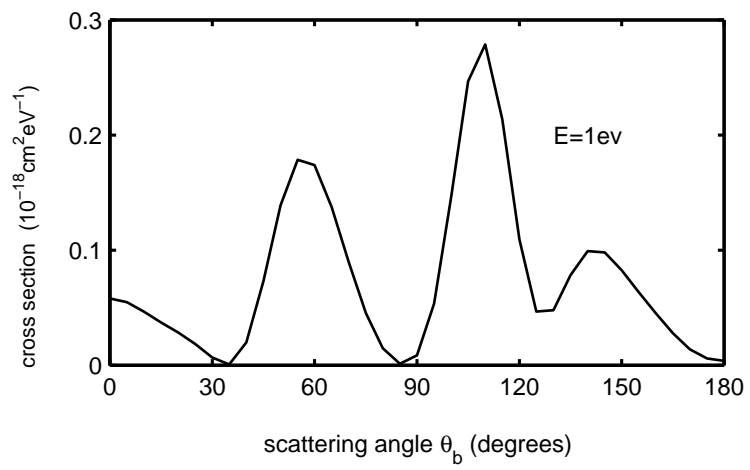


Figure 1(c)

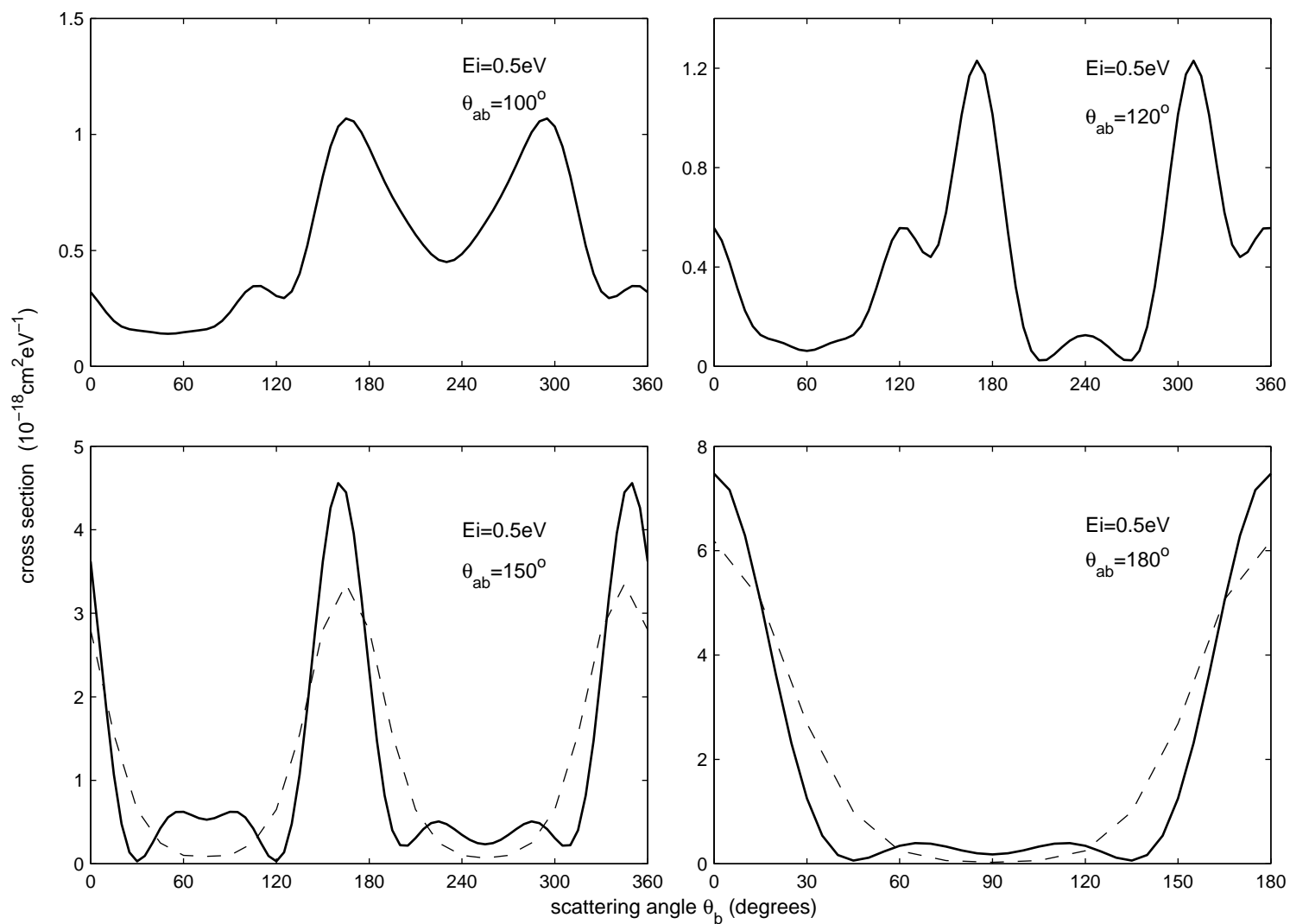


Figure 2(a)

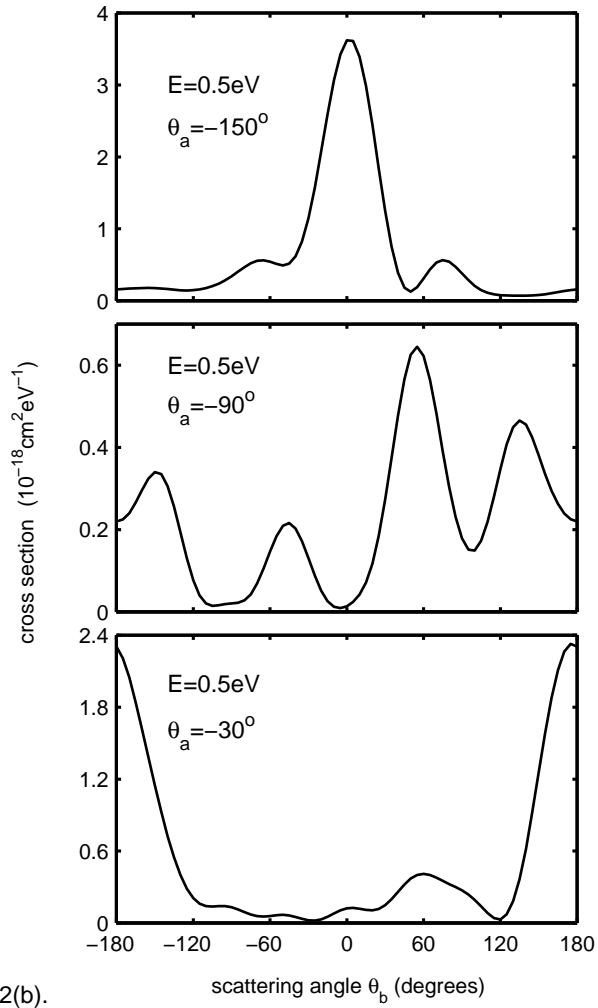


Figure 2(b).

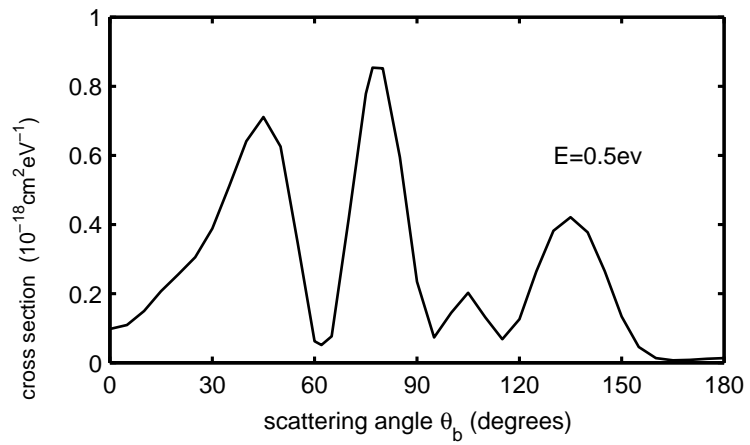


Figure 2(c)

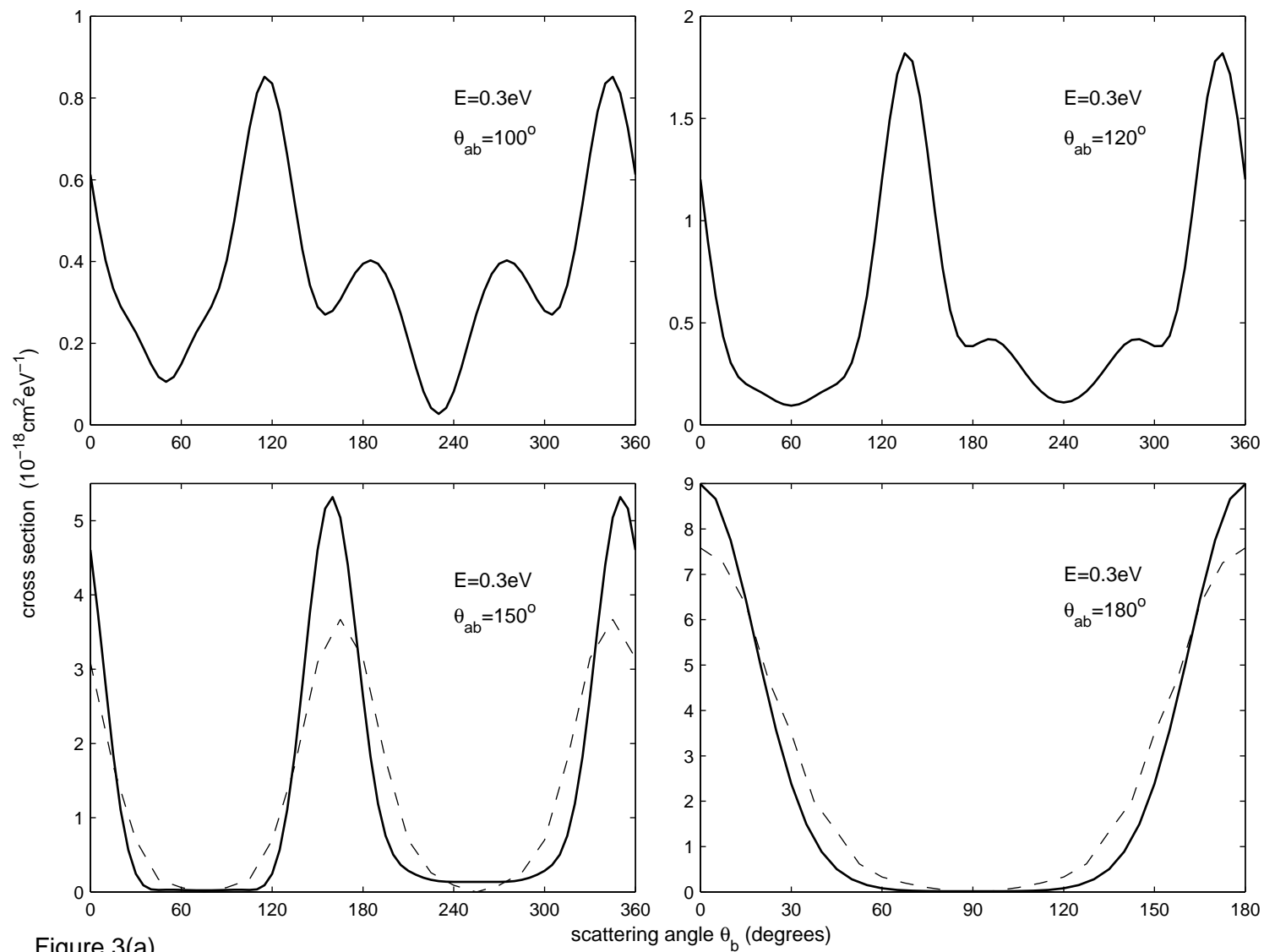


Figure 3(a)

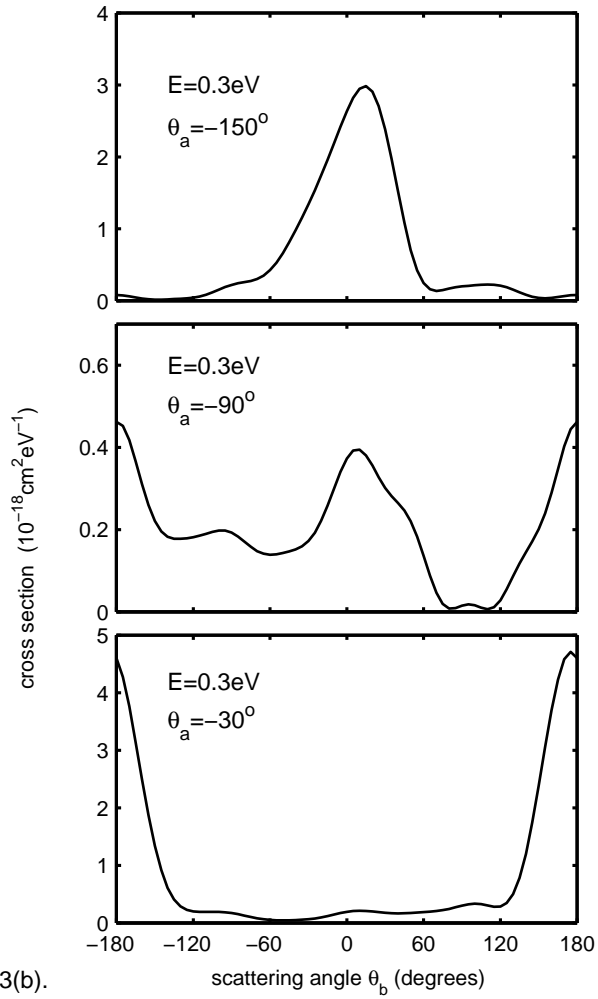


Figure 3(b).

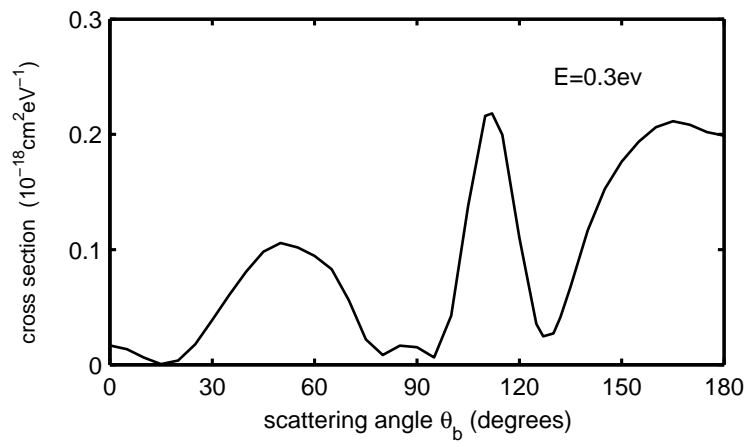


Figure 3(c)